Max-Planck-Institut
für biologische Kybernetik
Arbeitsgruppe Bülthoff

Spemannstraße 38 • 72076 Tübingen • Germany

Technical Report No. 035 July 31, 1996

# Evolution of the Sensorimotor Control in an Autonomous Agent

**Susanne A. Huber, Hanspeter A. Mallot, Heinrich H. Bülthoff**

## Abstract

Visually guided agents are introduced, that evolve their sensor orientations and sensorimotor coupling in a simulated evolution. The work builds on neurobiological results from various aspects of insect navigation and the architecture of the "Vehicles" of Braitenberg (1984). Flies have specialized visuomotor programs for tasks like compensating for deviations from the course, tracking, and landing, which involve the analysis of visual motion information. We use genetic algorithms to evolve the obstacle avoidance behavior. The sensor orientations and the transmission weights between sensor input and motor output evolve with the sensors and motors acting in a closed loop of perception and action. The influence of the crossover and mutation probabilities on the outcome of the simulations, specifically the maximum fitness and the convergence of the population are tested.

This document is available as `/pub/mpi-memos/` via anonymous ftp from `ftp.mpik-tueb.mpg.de` or from the World Wide Web, `http://www.mpik-tueb.mpg.de/projects/TechReport/list.html`.

# 1 Introduction

In this work autonomous agents are introduced which navigate through a virtual world. Genetic algorithms are applied to evolve their visually guided control mechanisms and generate a sensorimotor coupling which enables them to survive in the environment. In particular, the behavioral module for obstacle avoidance is studied. For the task a visuomotor program is generated with the sensors and effectors acting in a closed loop of perception and action, thus effecting a permanent sensorimotor interaction.

In information processing the architecture of autonomous systems is decomposed into a chain of functional modules such as perception, information processing in a central unit and the execution and output of information. In other approaches the architecture is decomposed into task-achieving modules, which, in combination, produce the complex, "emergent" behavior of biological (Tinbergen, 1953) and artificial systems (Brooks, 1986; Flynn & Brooks, 1989). Starting from the assumption that perception and action – sensor input and motor control – did not develop independently from each other, but are a coupled system – they have to be investigated in a closed loop. Braitenberg demonstrated with his "Vehicles" that even with simple architectures, it is possible to conceive of autonomous agents that can exhibit complex emergent behavior.

By studying the behavior of insects and the underlying neural mechanisms (for review see Egelhaaf & Borst, 1993), the architecture of biological navigation systems has been investigated. For our agent, the most important biological insight is that insects navigate mostly by evaluating visual motion information by means of neurons tuned to specific motion patterns (matched filters). The spatial localization of the receptive fields of these neurons is optimized with respect to certain behavioral tasks.

Franceschini and his colleagues demonstrate that the principle of motion vision can be used for navigational tasks in simulated and real agents (Franceschini, Pichon & Blanes, 1992). Cliff, Husbands and Harvey (1994) show the efficacy of using genetic algorithms to evolve concurrently the visual morphology along with the control networks. Here, we attempt to combine these approaches by evolving a competence for obstacle avoidance through simultaneous adaptation of sensor parameters and the sensorimotor coupling.

In the section 2, results from the research on the visual system of flies are reviewed and in section 3 the architectures of two types of autonomous agents are described. In section 4 the genetic algorithms used here are introduced, followed by the results of the simulations.

# 2 Perception of motion and visuomotor control in flies

The resolution of the compound eyes of flies is much coarser than that of human eyes and thus the perception of shape is more difficult. Hence, for visual orientation the detection of motion plays a more prominent role. While the insect is navigating through a stationary environment the images on the retinae are continuously changing. This image flow depends on both the trajectory through the world and the structure of the environment. In a stationary environment the rotational flow field contains information about the egomotion only, whereas translational fields contain both information about the structure of the environment and information about the movement of the observer. Objects nearby cause a larger image flow than objects further away (Longuet–Higgins & Prazdny, 1980).

As a model for motion perception in insects, Reichardt & Hassenstein proposed a correlation detector (Hassenstein & Reichardt, 1956; Reichardt, 1961) which correlates temporal modulation of image intensities in two neighboring ommatidia. Here we use a version of the correlation-type movement detector, where the visual signals first are temporally highpass filtered, making the motion detector independent of background illumination. From the investigation of the behavior of flies under controlled experimental conditions (Götz, 1964; Reichardt, 1979) as well as with freely flying flies (e. g. Wehrhahn, Poggio, Bülthoff, 1982; Wagner, 1985), different visuomotor subsystems for course control and object fixation have been described. This behavior corresponds to anatomical structures that are located in the visual area of the fly's brain. The so–called tangential cells (Hausen, 1982) (in the lobular plate – a section of the visual system) are known to play a prominent role in the detection of egomotion and thus are essential for the visuomotor control that compensates for deviations from the intended course. One example is shown in Fig. 1 (Hengstenberg, Krapp, Hengstenberg (in press)). These cells have large receptive fields, which together cover most of the visual field.

A second system detects image expansion sig-

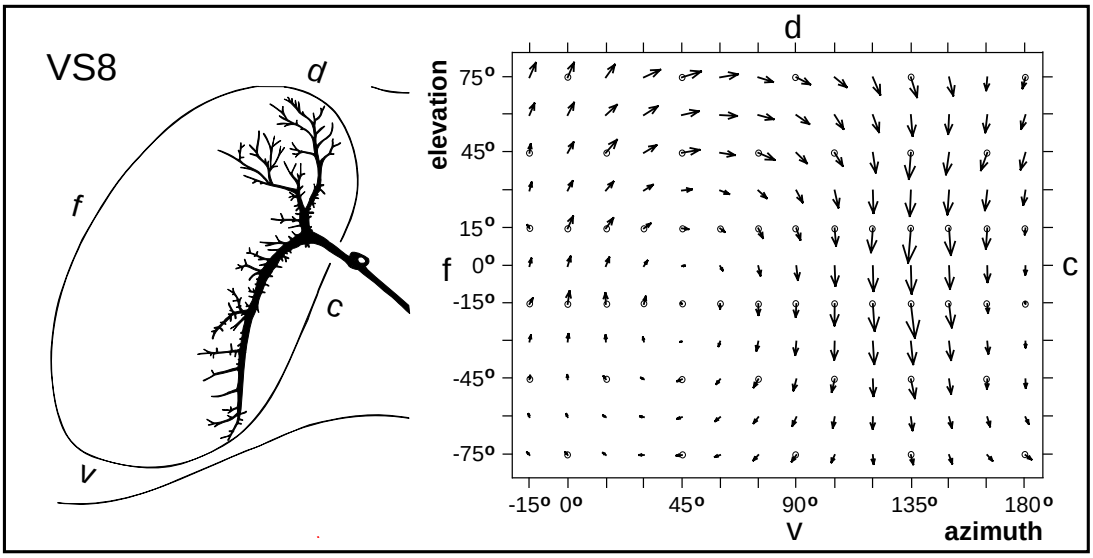


Figure 1: *Tangential cell VS8, responding maximal to rotations around the axis with azimuth* 45° *and elevation* −9°. *The measured flow vectors are indicated by a circle, the vectors in between result from interpolation (Hengstenberg et al. (in press)).*

nalling approaching objects or obstacles in the heading direction. Motion in small parts of the visual field which result from movements of small objects are detected by a third class of cells; it is used for the tracking of other flies (Egelhaaf & Borst, 1993). Position and extension of the receptive fields of these neurons in the visual system of the fly and also the specialization to certain motion patterns are essential for the course control of the fly.

## 3 The autonomous agents

In order to build an artificial agent that navigates using strategies as they are known in flies (see section 2), the idea is to evolve the matched filters and the sensorimotor coupling for certain behavioral tasks. In flies, each filter consists of a field of motion detectors with specialized orientations (Fig. 1). In this work we start with an agent that has only four visual sensors and two motors. Two sensors form a movement detector and the outputs of the two detectors are coupled via transmission weights to the two motors. The autonomous agent gathers information about its egomotion and the environment by evaluating the motion signals from the detectors. The orientations of the visual sensors determine which part of the motion field is used to navigate through the unknown environment.

They are thus a particularly simple case of matched filters for the course control. Genetic algorithms are used to evolve the sensor orientations and the coupling weights between sensors and motors for different types of behaviors.

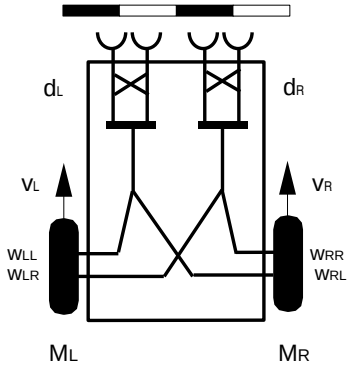


Figure 2: *The agent has four sensors, the orientations of which is given by the angles azimuth* $\Phi$ *and inclination* $\Theta$. *The outputs of these detectors* $d_L$ *and* $d_R$ *are connected to the motors* $M_L$ *and* $M_R$ *via the sensorimotor coupling.*

The input to each sensor is computed by "ray tracing" (Foley et al., 1987) where the intensities of single points – at the intersection of the line of sight with the visible surfaces – are averaged over a given number of sampling points. The orientations of the optical axes of the two sensors on one hemisphere of the visual field are evolved by the genetic algorithm. The other pair of sensors is positioned bilaterally symmetric on the other hemisphere. The time constants of the lowpass

filters of the correlation motion detector are fixed ($\tau_{LP1} = 2.0\text{s}, \tau_{LP2} = 5.0\text{s}$). The matrix

$$\mathbf{W} = \begin{pmatrix} w_{LL} & w_{LR} \\ w_{RL} & w_{RR} \end{pmatrix} \quad (1)$$

contains the transmission weights for the sensorimotor coupling of the outputs $d_L$ and $d_R$ of the two motion–detectors with the two motors $M_L$ and $M_R$. The velocity of the system is proportional to the force of the two motors, each motor producing a basic velocity $\mathbf{v}_0$ which is modulated by the visual information:

$$\begin{pmatrix} v_L \\ v_R \end{pmatrix} = \mathbf{v}_0 - \mathbf{W} \begin{pmatrix} d_L \\ d_R \end{pmatrix} . \quad (2)$$

The velocity $V$ in the heading direction and the anglular velocity are:

$$V = \frac{1}{2}(v_L + v_R) \quad \text{and} \quad \dot{\varphi} = \frac{v_L - v_R}{c} . \quad (3)$$

where $c = 10\text{cm}$ is the distance between the wheels. The system has two degrees of freedom: rotation around the vertical axis and translation in the heading direction. In the simulations the numerical accuracy is set to $10^{-6}$ simulating a small amount of noise.

### 3.1 Agent of type 1:

Here the angular aperture of each sensor is 10° azimuth × 10° elevation. We average the intensity of $10 \times 10$ sampling points to compute the visual input to each sensor. The basic velocity of the two motors is constant at $v_0 = 10\text{cm/s}$.
The agent moves through a tunnel which has a sinusoidal pattern ($\lambda = 1\text{m}$) mapped onto the walls, the floor and the ceiling. The width and height of the tunnel are 6m, the length is 100m. The elevation of the agent in the tunnel is kept constant at 3m. During evolution the system has to avoid two walls in the tunnel and maintain a safe distance of 15cm while navigating around the obstacles. The two walls are at $x = 15.0\text{m}$, $0.0\text{m} \le y \le 3.0\text{m}$ and $x = 35.0\text{m}$, $-3.0\text{m} \le y \le 0.0\text{m}$.

### 3.2 Agent of type 2:

For the agent of type 2 bilateral symmetry is assumed for the orientation of the motion detectors – as for agent of type 1 – and in addition for the transmission weights from the detector outputs to the motors. The angular aperture – being the same for all four sensors – is evolved. In order to keep the simulation time small, horizontal line sensors are used. The number of sampling points varies with the angular aperture of the sensors, the sampling base is kept constant at 1°. In addition the constant basic velocity $v_0$ of the two motors is a parameter optimized during evolution.
We run two blocks of simulations: in block 1 a sinusoidal pattern with the wavelength $\lambda = 2\text{m}$ is mapped onto the walls, ceiling and floor. Here the tunnel is 110m long and closed by a wall at both ends, the width and height is 4m. Four additional walls are placed at $x = 9\text{m}, 50\text{m}; 0.0\text{m} \le y \le 2.0\text{m}$ and $x = 19\text{m}, 80\text{m}; -2.0\text{m} \le y \le 0.0\text{m}$. The agent maintains a constant height of 2m.
In block 2 a random–dot pattern is used and walls are placed at $x = 9\text{m}, 50\text{m}; 0.0\text{m} \le y \le 2.0\text{m}$ and $x = 25\text{m}, 80\text{m}; -2.0\text{m} \le y \le 0.0\text{m}$. The tunnel is open at the end. The agents have to maintain a save distance of 10 cm from the walls.

## 4 Simulated evolution

### 4.1 The genetic algorithm

In a simulated evolution – using genetic algorithms – the autonomous agents adapt to the environment by generating an obstacle avoidance behavior. The orientation of two sensors and the transmission weights for the sensorimotor coupling are evolved. These parameters are encoded as a Gray-coded bitstring. Starting with a random initial population of bitstrings, each new generation is obtained by the following procedure:

1. Raw fitnesses are scaled linearly such that average fitness $\bar{f}$ is unchanged and maximal fitness is scaled to $n\bar{f}$ for some constant $n \ge 1$ (Goldberg, 1989). The coefficient $n$ is set to:
$$n = \min\{n_c, n_0\} \quad (4)$$
where $n_c$ is a constant value and
$$n_0 = \frac{f_{\max} - f_{\min}}{\bar{f} - f_{\min}}. \quad (5)$$
For the case $n_c > n_0$, scaling causes negative fitness values if $n_c$ is used. Therefore $n_0$ is applied instead. Here the scaling still leaves the average fitness $\bar{f}$ unchanged but leads to a scaled $f_{\min} = 0.0$ – preventing negative fitness values – and a scaled $f_{\max} = n_0\bar{f}$.
2. The number of offspring of each individual, $N_i$, is obtained by a random procedure such that the expectation of $N_i$ is proportional to the scaled fitness ("roulette–wheel" selection). In terms of the raw fitness, we have
$$E(i) = \frac{N-1}{N}(1 + (n-1)\frac{f_i - \bar{f}}{f_{\max} - \bar{f}}), \quad (6)$$
where $N$ is the total population size. The factor

$(N-1)/N$ is needed since only $(N-1)$ individuals of the new generation are obtained by this scheme.

3. The selected parents exchange their genetic material by one–point crossover. In addition point–mutation is used to introduce new genetic material into the population.
4. The individual with maximal fitness is transferred to the next generation automatically ("elitist–strategy"; Davis, 1991).

| | $C_{++}M_{+}$ | $C_{++}M_{0}$ | $C_{0}M_{+}$ | $C_{0}M_{++}$ |
|---|---|---|---|---|
| $p_c$ | 0.7 | 0.7 | – | – |
| $p_m$ | 0.01 | – | 0.01 | 0.1 |

Table 1: *Probabilities for mutation $p_m$ and crossover $p_c$ tuned by hand.*

### 4.2 Probabilities for mutation and crossover

The optimal parameter settings for the mutation and crossover probabilities are not yet fully understood. The genetic algorithms of Holland (1975) use crossover as the primary operator with mutation being of secondary importance. In general, mutation has a high exploratory power independent of the diversity of the population (Spears, 1993). The power of crossover lies in the construction and preservation of individuals of high fitness. The exploratory power of crossover is limited as the population loses diversity and the individuals become more and more similar. According to Spears (1993) the choice of the genetic operators depends on whether the whole population should gain a high fitness – here using crossover is of advantage – or one optimal individual is to be found, in which case use of mutation is sufficient to obtain comparable and better results. In order to test the optimization behavior of the genetic algorithm for different crossover and mutation probabilities ($p_c$ and $p_m$), we selected four conditions (see Table 1) in our first block of simulations.

### 4.3 GA 1

For the agent of type 1 the angles azimuth $\Phi$ and inclination $\Theta$ – describing the sensor orientations – are encoded with 4 bits each, in the range from 5° to 175° with a stepwidth of 11.3°. The weights of the sensorimotor coupling can take the eight real values $[\pm 0.5, \pm 0.1, \pm 0.05, \pm 0.01]$; they are encoded with 3 bits each. The length of the resulting bitstring is thus $4 \times 4\text{bits} + 4 \times 3\text{bits} = 28\text{bits}$.
The raw fitness $f$ is set to zero if the agent bumps into a wall within 400 time steps. Individuals which survive the 400 time steps in the tunnel without colliding with the walls, receive the fitness:

$$f = \frac{x(t=400)}{\dot{\varphi}_{\max}} \,. \tag{7}$$

Here $x$ is the component of the position on the center axis. Additionally, in order to keep the change in rotations in a limited range, the maximal angular velocity generated on the path $\dot{\varphi}_{\max}$ is used. A population size of 100 and $n_c = 1.2$ are used.

### 4.4 GA 2

The angles $\Phi$ and $\Theta$ of the agents of type 2 are again encoded with 4 bits each. The angular aperture is encoded with 3 bits in the range of 10.0° to 27.5° with a stepwidth of 2.5°. The transmission weights of the sensorimotor coupling can take real values in the range of [-0.38,0.38] and the basic velocity ranges from 5cm/s to 10cm/s in steps of 0.2 cm/s. The transmission weights and $v_0$ are encoded with 8 bits each. The length of the resulting bitstring is thus $4 \times 4\text{bits} + 1 \times 3\text{bits} + 3 \times 8\text{bits} = 43\text{bits}$.
The crossover and mutation probabilities are set according to the condition $C_{++}M_{+}$. Individuals which bump into a wall do not receive zero fitness as in GA 1. This is in order to support individuals that collide with a wall at a later time step. Collision here is punished by dividing the fitness they received at the point of collision by a factor of 2. A populationsize of 50 and $n_c = 2.0$ are used.

#### 4.4.1 Simulation block 1

The fitness function for the agent of type 2 in the simulation of block 1 is:

$$f = ksx_{max} \tag{8}$$

with $k = 1/2$ if the agent bumps into a wall and $k = 1$ if not. $s$ is the length of the path the agent covers, and $x_{max}$ the maximum value on the center axis of the tunnel the agent reached.

#### 4.4.2 Simulation block 2

Here the fitness function is:

$$f = k \sum_i |\Delta x_i| x_{max} \tag{9}$$

where $|\Delta x_i|$ is the distance on the center axis the agent covers in 10 steps. $|\Delta x_i|$ is computed every 10 steps and $x_{max}$ is again the maximum value on the center axis of the tunnel the agent reached.

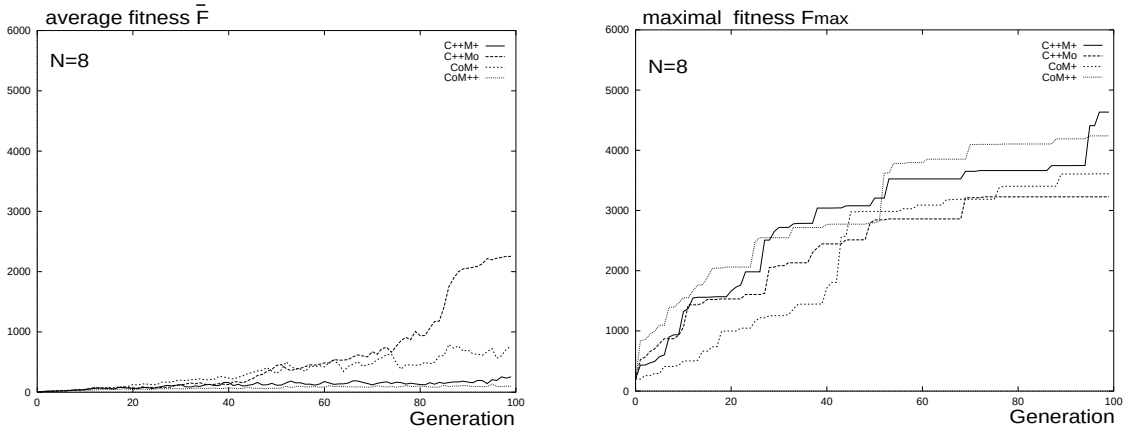


Figure 3: *Average (left) and maximal (right) fitness, averaged over 8 trials.*

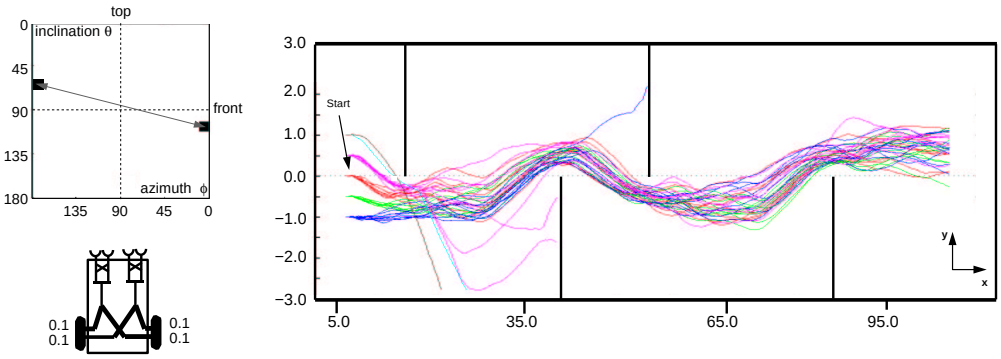


Figure 6: *Path in tunnel with 4 walls. Noise of* $\pm 10\%$ *is added to the input signals of the visual sensors and to the signals modulating the motor output. Even with different starting positions the agent travels through the tunnel in 93% of the trials successfully. Only in the extreme starting position* $y = 1.0$m *the agent bumps into the walls.*

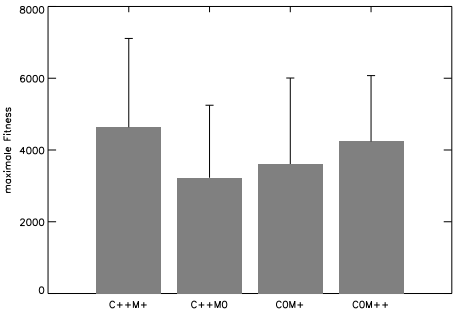


Figure 4: *GA 1: Maximal fitness at generation 100, averaged over 8 trials.*

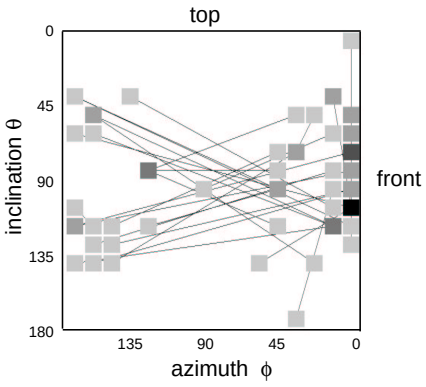


Figure 5: *Distribution of the orientations of the sensors for the best individual of each trial. The sensors forming a detector are connected by a line. The intensity of the sensors code the frequency of their occurrence, with darker greyvalues being more frequently.*

## 5 Simulations

### 5.1 Agent of type 1

In Fig. 3 the fitness $F_{\max}$ of the best individual and the average fitness $\bar{F}$ of the population for

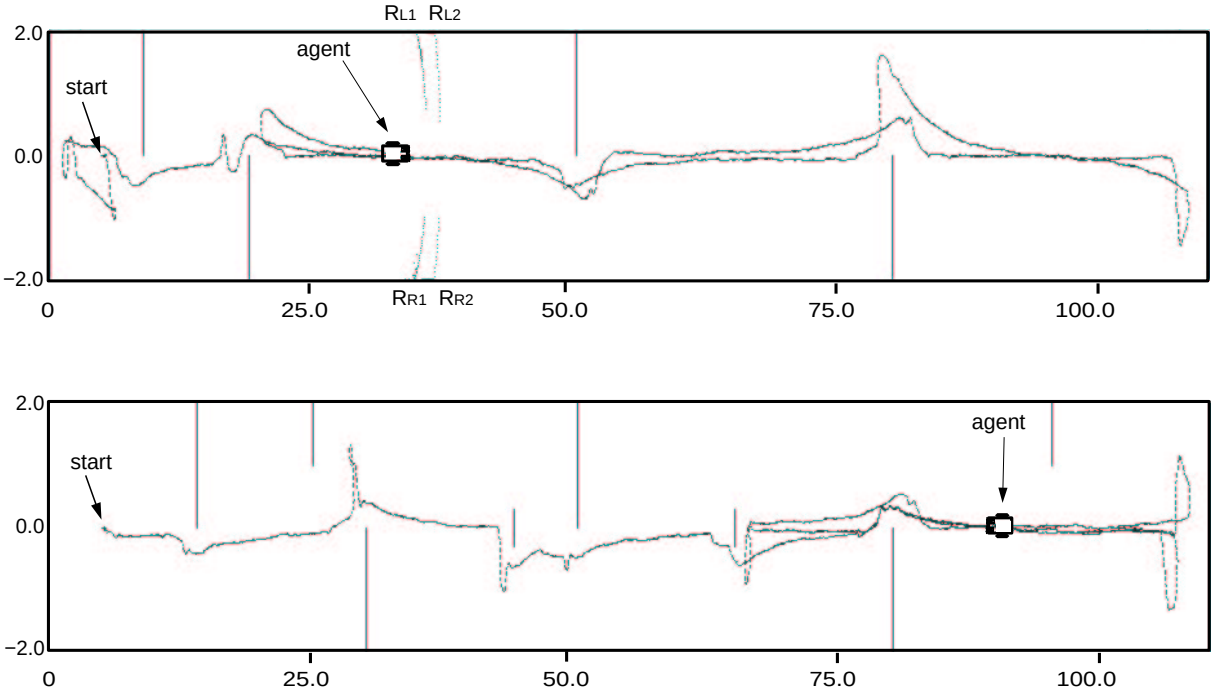


Figure 7: *Path in tunnel 1 (top) and tunnel 2 (bottom). $R_{R1}, R_{R2}$ and $R_{L1}, R_{L2}$ in tunnel 1 indicate the lines of intersection of the sensor rays with the walls of the tunnel. Noise of $\pm 10\%$ is added to the input signals of the visual sensors and to the motor output. Sinusoidal pattern is mapped onto the walls ceiling and floor ($\lambda = 2$).*

every generation, both averaged over 8 trials are shown. As a high proportion of the individuals bump into the wall and get zero fitness, the average fitness is much smaller than the maximum fitness for all four conditions. The maximal fitness after 100 generations averaged over 8 trials (see Fig. 3) is not significantly different between the different mutation and crossover probabilities. The average fitness $\bar{F}$ of the population is highest using only crossover followed by the $C_{++}M_{+}$ condition. The best individuals are obtained with the $C_{++}M_{+}$ condition.

One might expect that searching randomly for the optimal solution is faster than applying a genetic algorithm to this problem. Evaluating the fitness of 10,000 randomly chosen individuals only 0.68% travel through the tunnel without colliding with walls. The maximal fitness that is found with this technique is F=1310. This indicates that every 150th individual has a fairly well fitness when using the random search technique. With genetic algorithms a much higher fitness up to F=9331 is found.

The orientations of the sensors show a high variability (Fig. 5). Most of the agents evolve one sensor of each detector oriented in the heading direction, thus perceiving obstacles and the other sensor oriented towards the floor or ceiling of the tunnel or opposite to the heading direction. As long as there is no obstacle, correlating the two lowpass filtered sensor inputs leads to a symmetric detector output. With an obstacle detected in the front sensors an avoiding behavior is executed. The simulations are carried out with parameters for the mutation and crossover probabilities as described in Table 1. The motion detectors of the agent in Fig. 6 are oriented diagonal on the view sphere. One of the two sensors forming a detector on one hemisphere is oriented in the heading direction, the other backwards with an angular distance of 170°. The temporal change in the rotation angle here is $\dot{\varphi} = 0.2(d_L + d_R)/c$ deg/s. The velocity in the heading direction is $V = v_0$. Without obstacles the detector outputs are of equal magnitude, and due to the symmetric sensorimotor coupling the agent follows a straight line. A difference in the output of the movement detectors occurs if (i) the agent is not aligned to the center axis of the tunnel which leads to small turning reactions, (ii) obstacles appear in the field of view of the front sensor or (iii) the back sensor, with (ii) and (iii) causing large turning reactions in opposite directions. These three parts of the behavior enable the agent to avoid obstacles, starting with a large

turning reaction if the obstacle appears in the front sensor (ii) and aligning itself back to the center line of the tunnel (i) which is supported by (iii), when the obstacle appears in the back sensor.
This architecture enables the system to generalize the behavior to unknown environments. Here instead of two, four walls with different distances are used. They are placed at $x = 15.0\text{m}, 55.0\text{m}$, $0.0\text{m} \leq y \leq 3.0\text{m}$ and $x = 40.0\text{m}, 85.0\text{m}$, $-3.0\text{m} \leq y \leq 0.0\text{m}$. In order to test how robust this agent is, noise of $\pm 10\%$ was added to the visual input and to the signals modulating the motor output. Under this condition even with different starting positions ($y = -1.0, -0.5, 0.0, 0.5\text{cm}$) the obstacles are avoided in 93% of the trials successfully (Fig. 6). Only in the extreme starting position $y = 1.0\text{cm}$ the agent bumps into the walls.

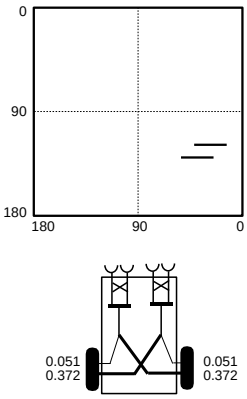


Figure 8: *The orientations of the two sensors forming a motion detector (the other two sensors are oriented symmetrically on the other hemisphere) and sensorimotor coupling for agent of type 2 resulting from the simulation of block 1.*

## 5.2 Agent of type 2

### 5.2.1 Simulation block 1

The agent of type 2 evolved in the simulation of block 1 (see Fig. 8) with the optical axes of its sensor orientations at 27.5° and 38.8° azimuth and 118.3° and 129.7° inclination. The evolved angular aperture of the sensors is with 27.5° much larger than for agent 1. The basic velocity of the motors is $\mathbf{v}_0 = 6.2\text{cm/s}$. The resulting angluar velocity is $\dot{\varphi} = -0.43(d_L + d_R)/c$ deg/s and the velocity in the heading direction $V = v_0 + 0.16(d_L - d_R)$ cm/s. With this architecture the sensors of an agent moving on the center axis receive visual input mainly from the floor and from a small part of the side walls. If the agent approaches an obstacle, response is smaller for the motion detector nearer to the obstacle. As the preferred direction of the motion detectors is almost vertical and the sinusoidal pattern is oriented vertically the walls and horizontally on the floor, the change of intensity in the sensors and thus the perceived motion decreases as the agent approaches an obstacle. The transmission weights for the contralateral connections are stronger than for the ipsilateral connections, hence the reduction of the detector output has a stronger effect on the velocity of the motor on the contralateral side and the agent turns away from the obstacle. The agents are tested in two different tunnels. Tunnel 1 is the original environment the agent evolved in, tunnel 2 differs in the number and position of the obstacles. Here we use 8 walls which are placed according to Fig. 7 (bottom). The test–trials are run with additional noise on sensor input and motor output. Table 2 describes the different noise conditions.
The agent has to survive 5000 time steps in the tunnel without bumping into a wall in order to show a successful behavior. With no additional noise the agent travels both tunnels in 100% of the time successfully. Adding more and more noise leads to a gradual reduction of performance. For tunnel 1 with $\pm 1\%$ noise, up to 70%–68% of the trials are successful, with $\pm 5\%$ 58–53 % and with a high noise of 10% still 46%–38% do not bump into a wall during 5000 time steps. For the tunnel 2 the performance is reduced to 44%–31% for the different conditions. In Fig. 7 examples of a successful travel through the tunnel 1 and tunnel 2 with 10% noise on sensor input and motor output are shown.

| | noise added to | |
|---|---|---|
| Condition | sensor input | motor output |
| s1 | $\pm 1\%$ | – |
| s5 | $\pm 5\%$ | – |
| s10 | $\pm 10\%$ | – |
| m1 | – | $\pm 1\%$ |
| m5 | – | $\pm 5\%$ |
| m10 | – | $\pm 10\%$ |
| s1m1 | $\pm 1\%$ | $\pm 1\%$ |
| s5m5 | $\pm 5\%$ | $\pm 5\%$ |
| s10m10 | $\pm 10\%$ | $\pm 10\%$ |

Table 2: *Conditions for noise testing.*

### 5.2.2 Simulation block 2

Here the agent evolves two sensors with the same inclination and overlapping receptive fields (Fig. 10). The optical axes are at 28° and 17°

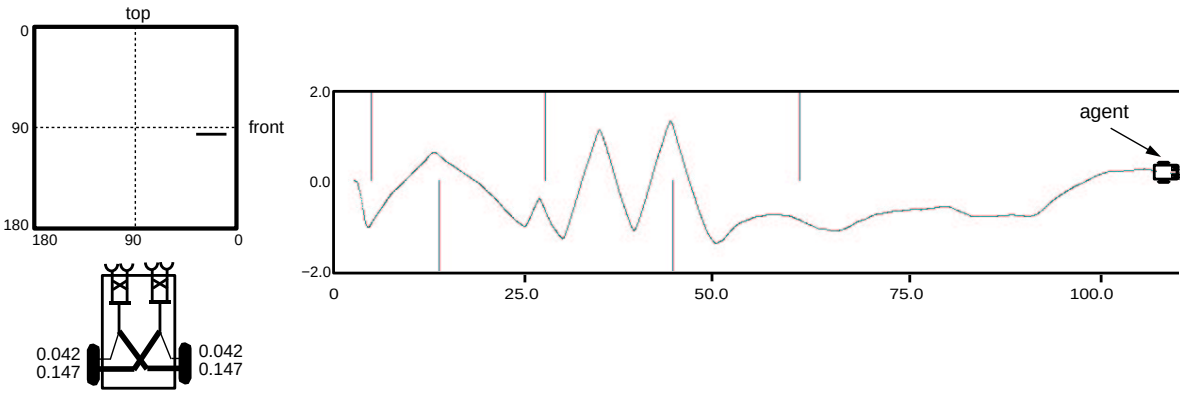


Figure 10: *The two sensors for agent 2 resulting from the simulation of block 2 on one hemisphere have overlapping receptive fields. Here their joint receptive field (top left) the transmission weights (bottom left) and the path in tunnel with 4 walls (right) are shown. A random dot pattern is mapped onto the walls, floor and ceiling.*

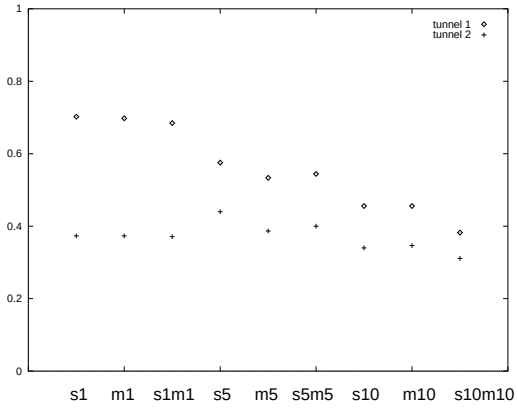


Figure 9: *Percentage of trials the individual of Fig. 8 travels tunnel 1 and tunnel 2 successfully. Noise according to table 2 is added.*

azimuth and 106° inclination. The angular aperture of one sensor is 15°. Covering the region between 9.5° and 35.5°. The basic velocity evolved to $v_0 = 6.4$cm/s resulting in an angular velocity $\dot{\varphi} = -0.19(d_L + d_R)/c$ deg/s and the velocity in the heading direction $V = v_0 + 0.05(d_L - d_R)$ cm/s. Here the preferred direction of the motion detectors is horizontal and thus with a vertical sinusoidal pattern on the walls the response of the motion detector is larger on the side where the obstacle is detected. Again the transmission weights for the contralateral connections are stronger than for the ipsilateral. Here the detected motion has opposite sign compared to the agent of block 1 and thus the velocity of the motor on the side contralateral to the obstacle is reduced and a turning movement away from the obstacle results. Test–trials with additional noise do not show a stable behavior. This might be due to the fact that a rotation of the agent caused by noise has a much higher influence on a motion detector system that has a preferred horizontal direction than on on a detector system oriented vertically, as rotations around the vertical axis cause horizontal image flow but leave vertical image flow unchanged. This has to be investigated in further experiments.

## 6 Summary and future work

Autonomous agents adapted to the tasks of obstacle avoidance behavior during a simulated evolution using genetic algorithms. The agents develop the viewing direction of their sensors and the sensorimotor–coupling in a closed loop and are thus able to compensate for deviations caused by external disturbances and to avoid obstacles in different environments. The influence of the crossover and mutation probabilities on the outcome of the simulations, concerning the maximum fitness and the convergence of the population was tested. In this experimental setup the average fitness of the population is highest if only crossover is used. Comparing the average maximal fitnesses obtained after 100 generations the use of crossover and/or mutation leads to comparable optimization results.

In future work we will evolve agents navigating in more complex environments. We plan to increase the number of movement detectors and use an array of sensors forming a 360° field of view. The agent will evaluate the motion detected in this field of view with filters that respond maximal to certain motion patterns – e.g. rotation around the vertical axis and translation in the direction of heading. Those filters are derived from the tan-

gential neurons (see sect. 2) found in the visual system of the fly's brain. In addition the agents will receive more degrees of freedom making 3D flight manoeuvers possible.

## 7 References


[1] V. Braitenberg. Vehicles – experiments in synthetic psychology. The MIT Press, Cambridge, MA, 1984.

[2] R. A. Brooks. A robust layered control system for a mobile robot. *IEEE Journal of Robotics and Automation*, RA-2: 14–23, 1986.

[3] L. Davis (ed.). Handbook of genetic algorithms. Van Nostrand Reinhold, New York, 1991.

[4] M. Egelhaaf, A. Borst. Motion computation and visual orientation in flies. *Comparative Biochemical Physiology*, 104 A/4: 659–673, 1993.

[5] A. M. Flynn, R. A. Brooks. Battling Reality. *MIT AI Memo 1148*, 1989.

[6] J. D. Foley, A. van Dam, S. K. Feiner, J. F. Hughes. Computer Graphics – principles and practice, Addison–Wesley, 1987.

[7] S. Forrest. Genetic Algorithms: Principles of natural selection applied to computation. *Science*, 261: 872–878, 1993.

[8] N. Franceschini, J. M. Pichon, C. Blanes. From insect vision to robot vision. *Philosophical Transactions of the Royal Society of London* B 337: 283–294, 1992.

[9] K. G. Götz. Optomotorische Untersuchung des visuellen Systems einiger Augenmutanten der Fruchtfliege *Drosophila*. *Kybernetik*, 2: 77–92, 1964.

[10] D. E. Goldberg. Genetic algorithms in search, optimization, and machine learning. Addison Wesley, Reading, Mass, 1989.

[11] I. Harvey, P. Husbands, D. Cliff. Seeing the light: Artificial evolution, real vision. *Proccedingsof the 3rd International Conference on Simulation of Adaptive Behavior*, 392–401, 1994.

[12] B. Hassenstein, W. Reichardt. Systemtheoretische Analyse der Zeit-, Reihenfolgen- und Vorzeichenauswertung bei der Bewegungsperzeption des Rüsselkäfers *Chlorophanus*. *Zeitschrift für Naturforschung*, 11b: 513–524, 1956.

[13] K. Hausen. Motion sensitive interneurons in the optomotor system of the fly. I. The horizontal cells: structure and signal. *Biological Cybernetics*. 45: 143–156, 1982.

[14] R. Hengstenberg, H. Krapp, B. Hengstenberg. Visual sensation of self-motions in the blowfly Calliphora. In: *Biocybernetics of Vision: Integrative and Cognitive Processes* (ed.) C. Taddei–Ferretti (in press).

[15] J. H. Holland. Adaptation in natural and artificial systems. The University of Michigan Press, Ann Arbor, 1975.

[16] H. C. Longuet–Higgins, K. Prazdny. The interpretation of a moving retinal image. *Proceedings of the Royal Society of London* B 208: 385–397, 1980.

[17] H. Mühlenbein. Evolution in time and space – the parallel genetic algorithm. *Foundations of Genetic Algorithms*, Morgan Kaufmann, San Mateo, CA, 1: 316 –337, 1991.

[18] W. Reichardt. Autocorrelation, a principle for the evaluation of sensory information by the central nervous system. In *Sensory Communication*: 303–317, ed: W. A. Rosenblith, The MIT Press and John Wiley and Sons, New York, 1961.

[19] W. Reichardt. Functional characterization of neural interactions through an analysis of behavior. In *The neurosciences, fourth study program*: 81–104, ed: F. O. Schmitt, The MIT Press, London, 1979.

[20] W. M. Spears. Crossover or Mutation? *Foundations of Genetic Algorithms*, Morgan Kaufmann, San Mateo, CA, 2:221–238, 1993.

[21] N. Tinbergen. Instinktlehre – vergleichende Erforschung angeborenen Verhaltens. Parey Verlag, Berlin, Hamburg, 1953.

[22] H. Wagner. Flight performance and visual control of flight of the free–flying housfly (*Musca domestica L.*), III. Interactions between angular movement induced by wide– and smallfield stimuli. *Philosophical Transactions of the Royal Society of London*, B 312: 581–595, 1986.

[23] C. Wehrhahn, T. Poggio, H. Bülthoff. Tracking and chasing in houseflies (*Musca*). *Biological Cybernetics*, 45: 123–130, 1982.